

Phase-Dependent Stability and Substrate-Induced Deactivation by Strong Metal-Support Interaction of Ru/TiO₂ Catalysts for the Hydrogenation of Levulinic Acid

Fang Liu,^[a] Jamal Ftouni,^[a] Pieter C. A. Bruijninx,^{*,[a, b]} and Bert M. Weckhuysen^{*,[a]}

The choice of support type has a profound influence on catalyst performance in liquid phase hydrogenation reactions, including the catalytic hydrogenation of biomass-derived levulinic acid (LA) to γ -valerolactone (GVL). Catalytic performance, including stability, of three Ru/TiO₂ catalysts, having a similar mean Ru metal nanoparticle size but supported on three types of TiO₂, namely P25, rutile and anatase, is evaluated by multiple reuse under batch reactor conditions. The catalysts' physicochemical properties before and after recycling are characterized by XRD,

STEM, TGA and FT-IR after CO stepwise adsorption. The results show that the deactivation seen for (mixed) anatase-supported catalysts in dioxane can be attributed to strong metal-support interaction (SMSI) rather than coke formation or metal sintering, with the rutile-based catalyst being more resistant against such support reduction. Notably, SMSI formation under the applied, relatively mild conditions only occurs in the presence of organic acids, such as LA or valeric acid.

Introduction

As part of the transition to a more sustainable chemical industry, the use of non-edible biomass as feedstock for the production of renewable chemical building blocks, or platform chemicals, is desired.^[1] Two platform molecules of particular potential are biomass-derived levulinic acid (LA) and γ -valerolactone (GVL), both of which received much attention given their relative ease of synthesis and manifold potential applications.^[2,3] Indeed, LA can be obtained in one step from lignocellulosic biomass by a simple hydrolysis process^[4] and can be converted to GVL in another single step, with GVL finding possible application as a green solvent,^[5] food additive^[6] and as intermediate for the production of bulk polymers and advanced biofuels.^[4,7]

The production of GVL by hydrogenation of LA has received much attention, having been extensively studied both in the gas and liquid phase and with different reductants, including molecular hydrogen, formic acid and alcohols.^[8–11] Numerous heterogeneous metal-based hydrogenation catalysts, such as Raney Ni and noble metals on oxidic and carbon supports were developed to mediate GVL synthesis.^[12–14] Of these, Ru based catalysts have shown particularly excellent hydrogenation capacity.^[15,16] In an early example, Manzer *et al.* assessed the

performance of 5 wt.% Ir, Rh, Pd, Ru, Pt, Re and Ni catalysts loaded on activated carbon in LA hydrogenation at 150 °C under 55 bar (H₂) in 1,4-dioxane as solvent and found Ru/C to perform best.^[17] Tan *et al.* showed that Ru/TiO₂ (P25) could convert LA into GVL (selectivity > 99%) with a turnover frequency as high as 7676 h⁻¹ under relative mild reaction conditions (70 °C, 40 bar H₂) with water as solvent.^[18] Luo *et al.* also demonstrated that Ru/TiO₂ (P25) exhibited good catalytic performance in terms of GVL generation even under harsh reaction conditions in the LA mimic 2-ethylhexanoic acid, as well as in neat GVL as solvent.^[19]

Next to productivity, long-term stability is equally important for a catalyst, but typically receives much more limited attention.^[3] When run in the liquid phase, the catalyst is exposed to highly polar, elevated temperature LA hydrogenation conditions, with the added difficulty of having an acidic substrate.^[4] As a result of these harsh conditions, catalysts can be expected to deactivate as a result of metal sintering, leaching, support collapse or destruction.^[20] In addition, reactive intermediates can polymerize to form carbonaceous deposits and biogenic or process-derived impurities can poison the catalyst, with both these processes also leading to deactivation.^[3]

While carbon-based supports are known to be stable under hydrothermal and acidic hydrogenation conditions,^[21–23] they cannot, however, withstand the high temperature, oxidative conditions required for catalyst reactivation by coke burn off.^[20] Indeed, metal oxide-based supports are more widely employed in industrial processes on account of their stability against such gas phase regeneration conditions. If such metal oxides are stable also under the liquid phase conditions typical for biomass conversion and platform molecule generation still needs to be firmly established, however, and will strongly depend on the actual severity of the process (e.g. solvent choice, temperature, pressure, atmosphere, pH, etc.). TiO₂, for

[a] F. Liu, Dr. J. Ftouni, Prof. Dr. P. C. A. Bruijninx, Prof. Dr. B. M. Weckhuysen
Inorganic Chemistry and Catalysis group
Debye Institute of Nanomaterial Science, Utrecht University
Universiteitsweg 99, 3584 CG, Utrecht (The Netherlands)
E-mail: p.c.a.bruijninx@uu.nl
b.m.weckhuysen@uu.nl

[b] Prof. Dr. P. C. A. Bruijninx
Organic Chemistry and Catalysis group
Debye Institute of Nanomaterial Science, Utrecht University
Universiteitsweg 99, 3584 CG, Utrecht (The Netherlands)

Supporting information for this article is available on the WWW under <https://doi.org/10.1002/cctc.201802040>

example, has been shown to resist aggressive aqueous media, especially hydrothermal and acidic hydrogenation conditions. For example, calculations showed (bulk) TiO_2 to be stable in hot water at 200 °C, over almost the entire pH range.^[20] Ru/TiO_2 (P25) was indeed found to maintain its catalytic activity and selectivity in LA hydrogenation in up to 6 batch recycling tests at 70 °C under 40 bar H_2 in water.^[18] TiO_2 has also shown good performance in other solvents, for example in a continuous flow screening study of the LA hydrogenation activity of 50 different supported noble metal catalysts, performed at 200 °C under 40 bar H_2 using LA dissolved in GVL as feedstock.^[4] Pt on TiO_2 (P25) proved to be 10 times more active than its SiO_2 and C counterparts, demonstrating a very stable GVL production (> 95 % selectivity) for up to 100 h time-on-stream.^[4] On the other hand, Abdelrahman *et al.* found that Ru/TiO_2 (P25) lost its catalytic activity with time-on-stream in LA hydrogenation at 50 °C under 24 bar H_2 in a continuous flow reactor with H_2O as solvent, deactivation being attributed to Ru sintering and coke formation rather than to changes in the TiO_2 support, however.^[13] Ftouni *et al.* also reported on the deactivation of a Ru/TiO_2 (P25) catalyst used for LA hydrogenation at 150 °C under 30 bar H_2 in dioxane, with activity gradually dropping upon batch recycling. Surprisingly, characterization of the reused catalysts showed that neither Ru sintering, leaching nor coke were responsible for deactivation, but rather Ru nanoparticle overcoating by reduced TiO_{2-x} species.^[24]

Indeed, the elevated temperature and reducing conditions employed in hydrogenation reactions can in principle present another stability challenge for reducible oxides such as TiO_2 . Such supports can suffer from noble-metal mediated H spillover onto the support, resulting in surface reduction and support rearrangement and ultimately coverage of the metal nanoparticle by the support, a phenomenon described as Strong Metal Support Interaction (SMSI).^[25–27] The SMSI concept was first developed by Tauster *et al.* in 1978 to describe the dramatic reduction in metal chemisorption ability seen for TiO_2 supported noble metal materials^[28] and has been extensively studied since then. For TiO_2 supported systems, such SMSI formation processes typically require elevated temperatures (above 300 °C) in a pure or dilute H_2 atmosphere.^[29,30] The mildest conditions we could find for such support reduction via SMSI with a Ru loaded TiO_2 (P25) catalyst were reported by Badyal *et al.*, showing support reduction and metal nanoparticle overcoating after a gas phase H_2 treatment at 250 °C for 2 h.^[31]

SMSI can exert different effects depending on the type of reaction.^[31,32] For instance, it has been documented that SMSI formation in TiO_2 supported catalysts benefited activity in the hydrogenation of carbonyl groups toward alcohols,^[33–36] nitrate reduction to nitrite^[37] and photocatalytic bio-hydrogen production from glucose solution.^[38] More often than not, however, the overcoat formed by the SMSI is considered detrimental for the activity of the metal phase and is best to be avoided.^[39,40] For example, Ko and Garten pointed out that TiO_2 supported group VIII metals always exhibited a much lower reactivity, up to several magnitude orders in ethane hydrolysis compared to their SiO_2 counterparts, due to SMSI formation when the catalyst was pre-reduced at 500 °C.^[41] Sa *et al.* demonstrated

with FT-IR that reduced CO uptake due to SMSI was already seen for Pd/TiO_2 catalyst after H_2 reduction at 200 °C. Upon increasing the reduction temperature to 350 °C, patches of a Ti_4O_7 phase on the Pd particles could be observed by TEM.^[25] In addition to high temperature H_2 reduction, surface decoration can also occur by vacuum treatment, for which, again, high temperatures are needed (e.g. 327–527 °C).^[26,42,43]

The deactivation of the Ru/TiO_2 catalyst during LA hydrogenation, as reported by Ftouni *et al.*, was also attributed to such an SMSI. Indeed, Ru nanoparticles were found to be blanketed by a disordered titania surface layer of 1–3 nm thick, as could be clearly seen by Aberration Corrected Scanning Transmission Electron Microscopy (AC-STEM) after repeated reuse.^[24] Compared to the above examples, the mode of deactivation was somewhat unexpected given the relatively mild hydrogenation conditions of 150 °C in dioxane.^[24] The underlying reasons for SMSI formation under such mild conditions remain to be elucidated.

The ease and extent of TiO_2 reduction, aided by SMSI or not, depend on the particular TiO_2 phase that is studied. Indeed, the vast amounts of studies dedicated to the generation of 'black' titania for photochemical/physical applications have shown that anatase reduces more readily than rutile.^[28,29] In addition, the type of TiO_2 support used has also been shown to have a pronounced effect on catalyst hydrogenation performance. For example, Hernandez-Mejia *et al.* used a series of Ru catalysts supported on different TiO_2 phases for the catalytic hydrogenation of xylose and found metal dispersion to depend on the titania crystal structure used, with a rutile supported Ru catalyst performing better than its anatase counterpart.^[44] Carballo *et al.* also noted that support structure, more than Ru precursor or support surface area determined Ru particle dispersion and further catalytic efficiency.^[45] Al-Shaal *et al.* compared the catalytic efficiency of rutile and P25 supported Ru catalysts in LA hydrogenation and found that no LA was hydrogenated over Ru/TiO_2 (rutile) in neither ethanol nor ethanol-water as solvent, whereas Ru/TiO_2 (P25) could produce GVL in good yields of up to 72%.^[23] The higher activity of the TiO_2 -P25 supported catalyst was thought to be the result of its higher surface area, facilitating either reactant adsorption or Ru dispersion.^[23] Ruppert *et al.* studied the effect of titania phase on LA hydrogenation in detail as function of rutile/anatase ratio and morphology.^[46] A high GVL yield was obtained with 20/80 and 10/90 rutile/anatase mixtures, while pure anatase supported catalysts were much less active. Activity was related to Ru dispersion and the electronic and surface properties of the two chosen phases.^[46] However, the examples available of titania phase-dependent LA hydrogenation performance give limited information on the influence of the type of TiO_2 support on the stability of the catalyst, including the support. For example, the extent to which the SMSI-induced support reduction is phase dependent is an open question.

In this work, we report on the influence of the type of TiO_2 support, rutile, anatase and P25 (mixture of anatase and rutile), on catalyst performance under typical liquid phase LA hydrogenation conditions in dioxane, with catalyst stability being assessed by multiply recycling tests. Catalytic activity and

characterization results show that the anatase(-containing) supported catalysts suffer from deactivation due to SMSI formation, whereas pure rutile is more stable against support reduction. Notably, support reduction (and by inference catalyst deactivation) by SMSI was found to be organic acid-induced, as it occurred only in the presence of the LA substrate or an added acid such as valeric acid.

Results and Discussion

Characterization of the Fresh Catalysts

To investigate the effect of TiO₂ phase composition on catalyst stability in liquid phase LA hydrogenation, three different types of TiO₂ (P25, anatase and rutile) were selected. 1 wt.% Ru/P25 and Ru/Rutile were prepared by wet impregnation with Ru(NO₃)₃ followed by calcination and high temperature (450 °C) reduction according to the method reported by Ftouni *et al.*^[24] The Ru/Anatase catalyst was instead prepared following the report of Piskun *et al.*^[47] in which RuCl₃·xH₂O is used as precursor followed by direct H₂ reduction. These methods were selected in order to obtain similar mean Ru particle sizes, of around 2.0–2.5 nm (see below), allowing any particle size effects on performance and deactivation to be discarded. The physicochemical properties of the fresh (and recycled) catalysts are summarized in Table 1, showing BET surface areas of the fresh

Table 1. Physicochemical properties of the fresh and spent TiO₂ supported Ru catalysts.

		BET [m ² /g]	Metal particle size [nm]	TGA [%]
Ru/P25	Fresh	75	2.5 ± 0.9	ND ^[a]
	Spent 5x Recycled	46	2.5 ± 1.0	0.3
	Spent Without LA	70	2.6 ± 1.4	0.3
	Spent With Valeric Acid	40	2.2 ± 1.1	ND
Ru/Rutile	Fresh	25	2.3 ± 0.8	ND
	Spent 5x Recycled	23	2.3 ± 0.9	0.6
Ru/Anatase	Fresh	11	2.0 ± 0.6	ND
	Spent 5x Recycled	12	3.1 ± 2.7	0.3

[a] not determined.

P25, anatase and rutile supported materials of 75, 11 and 25 m²/g, respectively. The characteristic diffraction peaks seen by XRD for Ru/Rutile and Ru/Anatase showed them to be phase pure, while, diffraction signals of both the anatase and rutile phases were observed for Ru/P25, with an anatase:rutile ratio of 80:20 (Figure S1). No Ru diffraction peaks were observed in the XRD patterns of any of the three Ru-based catalysts, indicative of the low loading and small Ru particle size. Figure 1 shows the TEM images and Ru particle size distribution for all three fresh Ru catalysts. The mean Ru particle diameters of Ru/P25, Ru/Rutile and Ru/Anatase were found to be similar ranging from 2.5 ± 0.9 nm, 2.3 ± 0.8 nm and 2.0 ± 0.6 nm, respectively. As can be viewed in the TEM image of the freshly reduced Ru/P25 catalyst, two differently shaped crystalline phases can be

observed. The rectangular-shaped fragments are identified as rutile and the smaller, round fragments as anatase, in line with the observation of Ohno *et al.* that the particle size of rutile in Degussa P25 is about four times larger than that of its anatase component.^[48] The TEM images furthermore showed that Ru was not found to be equally well dispersed over all titania crystallites in the Ru/P25 catalyst. Indeed, the majority of the Ru particles were located on the rutile phase (Figure 1a), in line with the observation of Ruppert *et al.*, who prepared a Ru/TiO₂ (P25) via incipient wet impregnation from Ru(acac)₃.^[46] In our case, a small portion of Ru particles was also found on the anatase component (Figure 1a, yellow round circle). On the other hand, the TEM images of the Ru/Anatase and Ru/Rutile samples showed a homogeneous distribution of Ru particles over the support.

FT-IR analysis after CO adsorption is a powerful method to monitor active metal surface properties of the catalyst, such as the oxidation state and degree of dispersion.^[49] Figure 2 shows the FT-IR spectra of the fresh catalysts after CO adsorption at liquid nitrogen temperature. A series of characteristic CO–Ti species is seen, in line with the results reported by Hadjiivanov *et al.*^[50] The low intensity bands centered at 2208 and 2190 cm^{−1} were attributed to CO interacting with electrophilic, pentacoordinated Ti⁴⁺ α and five-coordinated β' sites, respectively. At higher CO coverage, a gradual red shift from 2190 cm^{−1} to 2180 cm^{−1} is seen, as next to the CO–β' sites also the β'' sites adsorb CO. With increased CO pressure, one more kind of Ti⁴⁺ site, i.e. five-coordinated Ti⁴⁺ cations (γ sites) of very low acidity, was detected as well at around 2160 cm^{−1}.^[50] The bands centered at 2150–2155 and 2140 cm^{−1} were attributed to CO adsorbed on surface OH groups and physisorbed CO, respectively.^[51] That a CO–OH band (~2150 cm^{−1}) was absent for the Ru/P25 sample is indicative of the high degree of surface dehydroxylation after outgassing at 550 °C, whereas a large amount of residual hydroxyl groups were still present on the surfaces of Ru/Rutile and Ru/Anatase after annealing.^[52] In addition, broad bands centered at 2040, 2043 and 2046 cm^{−1} were observed for Ru/P25, Ru/Rutile and Ru/Anatase, respectively, assigned to CO linearly adsorbed on metallic Ru particles.^[53]

Catalyst Performance and Recycled Catalyst Characterization

The standard reaction conditions for LA hydrogenation in 1,4-dioxane as solvent consisted of a run at 150 °C under 30 bar H₂ in a batch autoclave, with catalyst stability first being assessed by multiple recycling tests. The results are summarized in Figure 3. GVL is the only product detected after reaction, no intermediates such as α-angelicalactone or GVL overhydrogenation products (e.g. 1,4-pentanediol and valeric acid) were observed. As the mass balance of substrate and products (LA + GVL) was always higher than 95%, as determined by GC analysis, only GVL yields are given below to compare catalytic activity between runs. The production of GVL as a function of

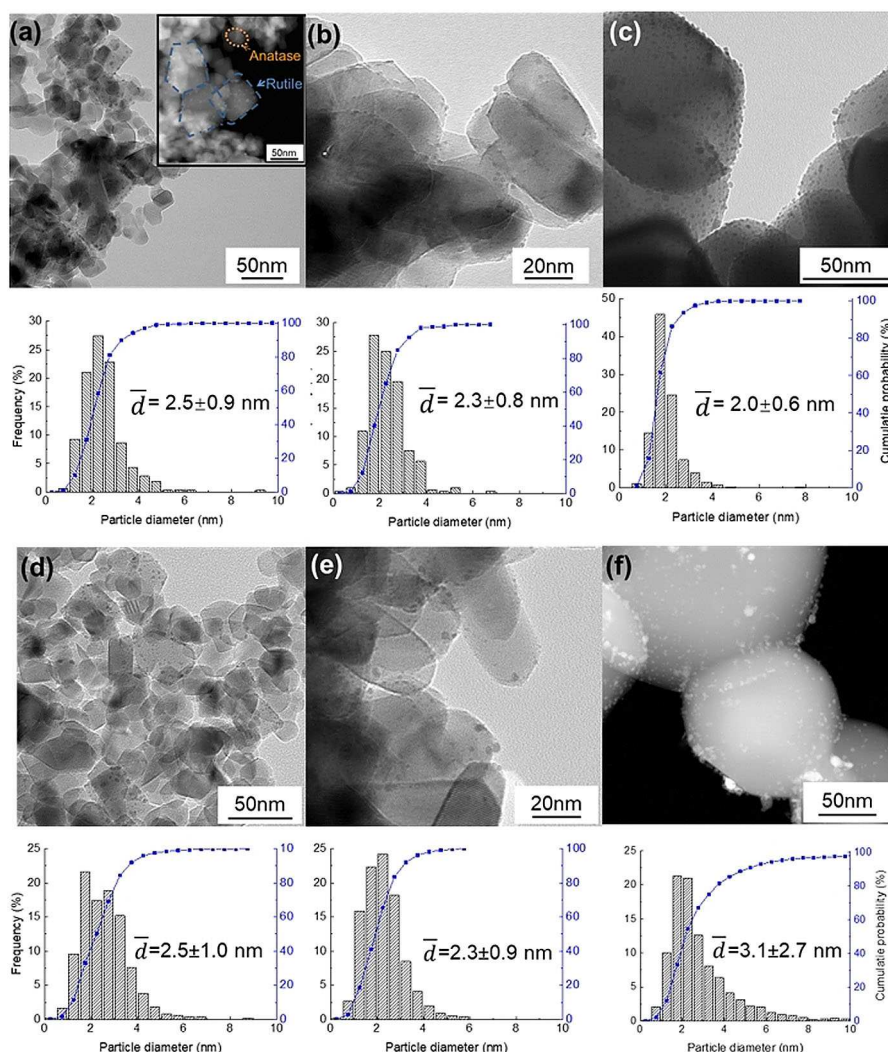


Figure 1. TEM images and Ru particle size distribution of fresh (a) Ru/P25, (b) Ru/Rutile and (c) Ru/Anatase, and 5 times reused (d) Ru/P25, (e) Ru/Rutile and (f) Ru/Anatase.

time (Figure 3a) varied in the following order: Ru/Anatase > Ru/Rutile > Ru/P25. This trend is different from a previous observation that a P25-based catalyst was more reactive than a rutile-based one in the LA hydrogenation in ethanol.^[23]

The production of GVL for the three catalysts under study as a function of recycle number is presented in Figure 3b, c and d. In line with previous observations,^[24] Ru/P25 deactivated upon recycling, showing a considerable drop in GVL yield from 69% to 24%, again as previously, attributed to a detrimental SMSI (see discussion below). Likewise, GVL yield over Ru/Anatase was also found to steadily decrease from full conversion to 49% after the 5th recycle. To properly see any deactivation in the first runs, recycling tests were also performed at lower conversion (LC), using a higher LA/Ru ratio. The results again show the pure anatase support to exhibit similar behavior to the anatase-rutile mixture (P25), with the yield gradually going down upon reuse. In contrast, Ru/Rutile proved to be more stable in term of GVL production upon recycling. GVL yield over Ru/Rutile

actually first went up to the third run to eventually drop upon further recycling.

To get further insight into the differences in catalyst behavior seen upon recycling, the five-times recycled Ru/P25, Ru/Anatase and Ru/Rutile catalysts were recovered and characterized. XRD analysis confirmed that the bulk titania phase composition did not change upon recycling (Figure S1), giving an identical anatase:rutile ratio of 80:20 for Ru/P25 before and after reuse. N₂ physisorption measurements showed a dramatic difference, however (Table 1). The recycled Ru/P25 showed a drop of ~40% in surface area compared to its fresh counterpart. A similar drop in surface area had been seen before for Ru/TiO₂ (P25) upon recycling and was attributed to support reduction and partial (surface) amorphization.^[24] Instead, almost no change in surface area was seen for both Ru/Rutile and Ru/Anatase. TGA analysis revealed weight losses of 0.3%, 0.6% and 0.3% for the recycled Ru/P25, Ru/Rutile and Ru/Anatase materials (Table 1), respectively, indicating coke formation is limited. The mean Ru particle size in Ru/P25 and Ru/Rutile

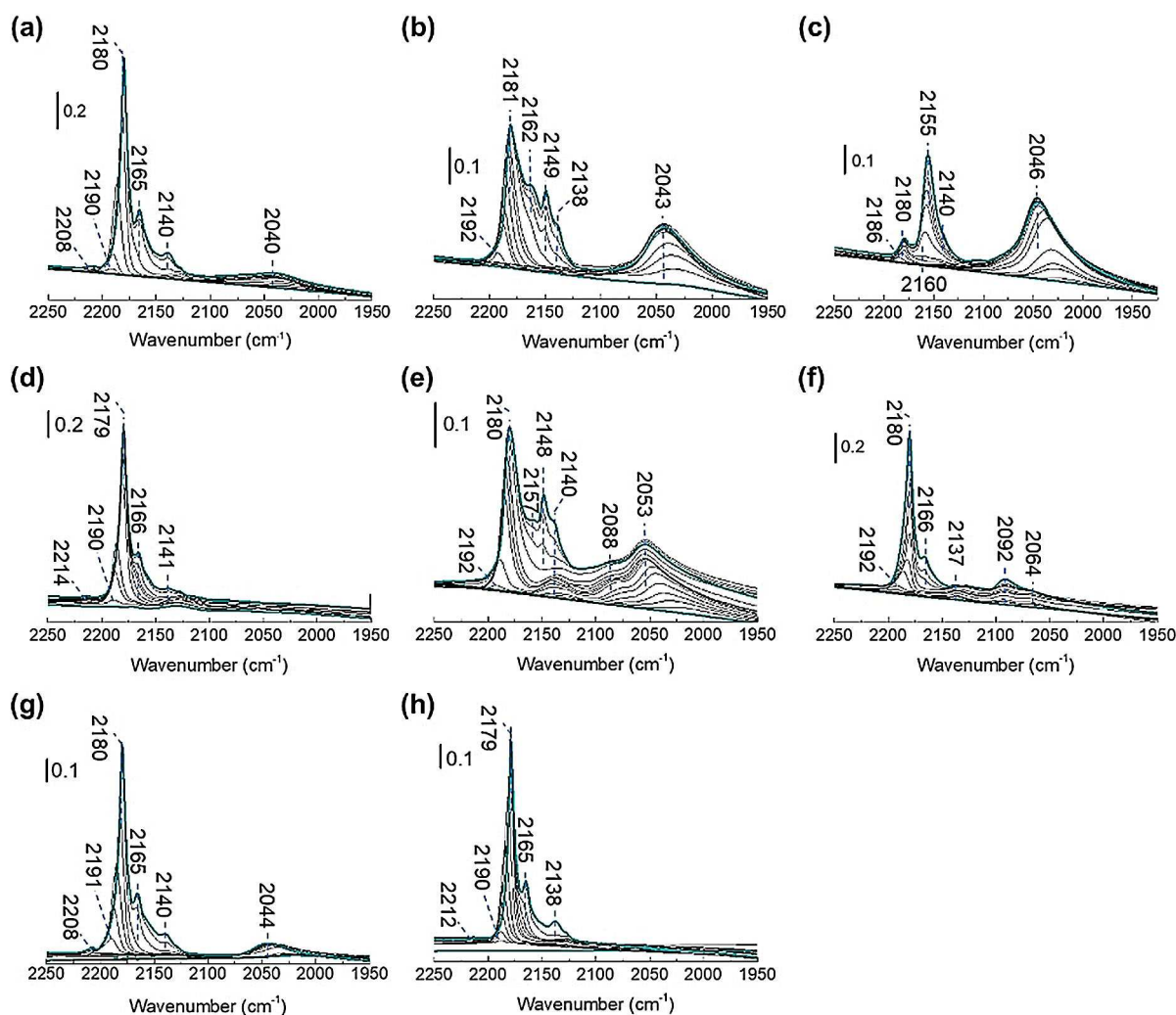


Figure 2. CO-FT-IR spectra of (a) fresh Ru/P25, (b) fresh Ru/Rutile, (c) fresh Ru/Anatase; (d) reused Ru/P25, (e) reused Ru/Rutile, (f) reused Ru/Anatase after five recycling tests after CO adsorption as function of pressure at -188°C ; (g) Ru/P25 treated without LA and (h) Ru/P25 treated with valeric acid under H_2 (30 bar) for 18 h after CO adsorption as function of pressure at -188°C . The spent catalysts were washed with acetone prior to the CO-FT-IR measurements.

remained the same before and after recycling, whereas some sintering was observed for Ru/Anatase with average Ru particle size increasing from 2.0 ± 0.6 nm to 3.1 ± 2.7 nm (Table 1 and Figure 1). TEM image of the five-times recycled Ru/P25 showed the Ru particles to be still preferentially deposited on the rutile phase (Figure 1d). ICP analysis demonstrated no detectable levels of Ru in the reaction solution, showing leaching to be very limited as well. Taken together, these results suggest that the observed phase-dependent deactivation of the Ru/TiO₂ catalysts is not linked to metal particle growth, leaching or the result of coke deposition.

Figure 2d–f show the FT-IR spectra of the recycled Ru catalysts after CO adsorption at liquid nitrogen temperature. After five recycle runs in dioxane, the CO-Ru⁰ signal clearly vanished in the spectrum of recycled Ru/P25, in line with the results (obtained for a three times reused Ru/P25) reported by Ftouni *et al.*^[24] Given the limited coke formation and Ru metal sintering, this decrease in CO adsorption ability is thought to be characteristic of SMSI formation.^[30] Indeed, it was previously

shown by AC-STEM that the TiO₂ (P25) support developed a continuous disordered surface layer of reduced Ti species varying in thickness between 1 and 3 nm after three cycles^[24] under LA hydrogenation reaction conditions similar to the one used here, the difference being the larger number of recycling steps and the higher LA/Ru ratio. A similar, nearly full decrease in CO adsorption on Ru was also observed for the 5-times recycled Ru/Anatase catalyst, again pointing at loss of adsorption capacity as a result of SMSI. Although some Ru sintering did occur upon recycling, this is not considered sufficient to account for the severe loss on CO adsorption of recycled Ru/Anatase catalyst. Indeed, we found that a five-times recycled anatase catalyst used in water rather than dioxane, despite having a much larger Ru mean particle size of 4.1 ± 4.7 nm, showed a better CO adsorption ability than its dioxane-recycled anatase counterpart (particle size 3.1 ± 2.7 nm) (data not shown). Therefore, the significant loss of CO adsorption capacity observed for the dioxane-recycled anatase catalyst is also most likely attributed to Ru surface coverage by SMSI formation. In

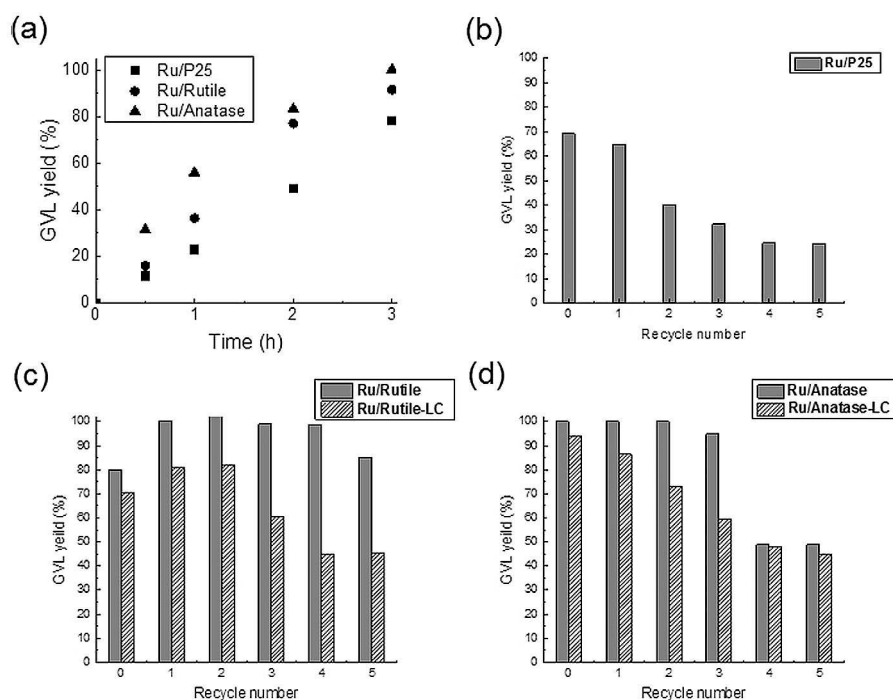


Figure 3. (a) GVL yield as function of reaction time, GVL yield as a function of recycling number for (b) Ru/P25, (c) Ru/Rutile and (d) Ru/Anatase in dioxane. Experimental conditions: $T = 150^{\circ}\text{C}$, $P(\text{H}_2) = 30$ bar and $t = 3$ h, $\text{LA}/\text{Ru} = 1400$; $\text{LA}/\text{Ru} = 3300$ for Ru/Rutile LC (low conversion) and Ru/Anatase LC recycle.

line with this, as a result of SMSI formation, the peak centered at 2155 cm^{-1} related to CO–OH adsorption seen in the fresh catalyst, was absent after recycling of Ru/Anatase, as also seen previously.^[54–56] Indeed, Chen *et al.* found H_2 -reduced black TiO_2 material to exhibit much less surface hydroxyl groups compared to pristine, white TiO_2 .^[55] Likewise, no band related to OH adsorption was observed in the CO-FT-IR spectrum of hydrogenated TiO_2 nanocrystals obtained after gas phase H_2 reduction (5 bar) at 450°C for 4 h, whereas clear CO–OH bands were detected with the untreated TiO_2 nanocrystals.^[54] Disordered surfaces were also seen for these two reduced titanias. In contrast, considerable peak intensity associated with CO adsorbed on Ru was still observed for Ru/Rutile after five times recycling, suggesting that pure rutile is more stable against support reduction than a (mixed) anatase phase. A similar conclusion was drawn by Li *et al.* using Electron Paramagnetic Resonance (EPR) as a means to compare the extent of SMSI formation for anatase and rutile supported palladium catalysts. Irreversible support reduction was observed for anatase, but not for a rutile supported catalyst after gas phase H_2 reduction at 200°C .^[29]

Notably, two new bands appeared centered at $2137/2140$ and $2092/2088\text{ cm}^{-1}$ in the FT-IR spectra of the recycled Ru/Anatase and Ru/Rutile catalysts, respectively, associated with CO species tightly bound to Ru, as they were stable upon high vacuum desorption (Figure S2).^[57] These band positions are very similar to those observed by Robbins, who attributed these to $(\text{TiO})_2\text{Ru}(\text{CO})_3$ surface species based on a CO-induced oxidation experiment on fully reduced Ru/ TiO_2 at 37°C ,^[58] indicating $\text{TiO}_{2-x}\text{-Ru}$ ligand formation after recycling. De la Peña O'Shea

et al. demonstrated that such amorphous Ti-metal mixed species were also generated in a related system as a result of SMSI formation. Layers of TiO_x moieties of a few atoms thick were detected on the surface of a Co/ TiO_2 catalyst after H_2 reduction at 500°C , indicative of SMSI surface decoration. These layers were accompanied by the formation of Co–O–Ti linkages as suggested by XPS analysis^[59] and the reduced Ti species were proposed to be stabilized by reaction with reduced cobalt, giving rise to an amorphous mixed oxide on the catalyst surface.^[59] Based on the work of Robbins^[58] and De la Peña O'Shea *et al.* ^[59], it can be inferred in our case that the appearance of these bands at high frequency support the evolution of surface $\text{TiO}_{2-x}\text{-Ru}$ species resulting from SMSI.

Summarizing, the above experiments show that the choice of TiO_2 support has a big influence on catalyst performance in dioxane. Under typical LA hydrogenation conditions, the reactivity of the anatase-supported catalyst outperforms the rutile one, which in turn shows better performance than the P25 catalyst. Upon recycling, (mixed) anatase catalysts show a fast and continuous deactivation in terms of GVL production, whereas, an initial jump in catalytic activity is observed for the rutile phase supported catalyst. Differences in ease of reducibility and resulting extent of SMSI seem to be the origin of these support effects. The CO adsorption ability is significantly depressed for P25 and anatase supported catalysts after recycling as revealed by the CO-FT-IR spectra, whereas considerable CO–Ru adsorption intensity is still observed for recycled Ru/Rutile, making the latter support more stable against deactivation under dioxane LA hydrogenation conditions.

Adsorbate-Induced Strong Metal Support Interaction

Under gas phase reduction conditions, support reduction by H₂ spillover is considered the main reason for SMSI formation.^[60] In this mechanism, adsorbed H₂ is dissociated by the supported metal, spilled over onto the TiO₂ support that gets reduced to TiO_{2-x} suboxides that eventually migrate over the surface of the metal particles. Such processes, however, typically require an elevated temperature ($\geq 250^\circ\text{C}$) in a pure or diluted H₂ gas atmosphere.^[29] In our case, the Ru/TiO₂ materials are exposed to much milder liquid phase conditions (150 °C), yet still suffered from deactivation by SMSI as demonstrated above. As we had already previously observed SMSI formation for the Ru/P25 material and again noted here strong deactivation for this material, we choose this particular material to further study the factors inducing SMSI in the liquid phase in more detail.

To test the role of H₂ alone on SMSI formation for the Ru/TiO₂ catalysts under mild liquid hydrogenation conditions, fresh Ru/P25, without LA substrate, was treated in an H₂ saturated dioxane solution (30 bar) at 150 °C for 18 h, equivalent to the time the catalyst was exposed to reducing conditions over the five recycle runs. Surprisingly, no evidence of SMSI was observed for the spent Ru/P25 material obtained after this run. N₂ physisorption revealed that the surface area of this spent catalyst is similar to that of fresh Ru/P25 (Table 1), while the CO-FT-IR spectrum of this treated Ru/P25 showed the CO-Ru⁰ vibration to be comparable to the fresh counterpart (Figure 2g), suggesting spent Ru/P25 did not lose its CO adsorption ability. These results suggest that LA may actually itself be involved in catalyst deactivation by SMSI.

Indeed, previous studies have shown that formic acid and generated formates adsorbed on TiO₂ support can give rise to an Adsorbate-induced SMSI state (A-SMSI) under relatively mild conditions.^[40,61,62] For example, Rui *et al.* found SMSI to occur not only upon high temperature H₂ reduction of Pt/TiO₂, but also when an as-calcined TiO₂ catalyst was reduced by a 35 wt.% formic acid water solution at 70 °C without any H₂ present. Very recently, such an adsorbate-mediated SMSI was also reported by Matsubu *et al.*,^[40] who found that, depending on the reaction and pretreatment conditions, a reduced Rh/TiO₂ catalyst could be blanketed by a thin, yet permeable support layer after appropriate treatment under 20% CO₂/2% H₂ at 250 °C. High coverage of HCO_x species was observed by *in-situ* DRIFT spectroscopy and, after comparison to formic acid decomposition on TiO₂, these HCO_x were held responsible for oxygen vacancy formation and for driving the A-SMSI.

To determine the effect of having an organic acid on SMSI formation under liquid hydrogenation conditions, a non-reducible acid, valeric acid, was used instead of LA and reacted with fresh Ru/P25 under the same acid/Ru ratio under 30 bar H₂ in dioxane for 18 h. No pressure drop was observed during the reaction, indicating that indeed no hydrogenation reaction occurred. The surface area of this spent catalyst dropped to 40 m²/g, comparable to the five-time recycled Ru/P25 after the LA runs (46 m²/g). TEM analysis confirmed that the mean Ru

particle size before and after valeric acid treatment was the same (Table 1). However, no CO-Ru⁰ vibration was anymore seen in the CO-IR spectrum of the recovered Ru/P25 material (Figure 2h), again similar to Ru/P25 after repetitive LA runs and indicative of A-SMSI. Matsubu *et al.* pointed out that different surface properties were observed for A-SMSI and traditional SMSI overlayers.^[40] Unlike the crystalline fully reduced metal-oxide layer observed for traditional SMSI, an amorphous and partially reduced metal-oxide overlayer was formed in the A-SMSI state, in line with our previous observations on the AC-STEM images of three times recycled Ru/P25 catalyst.^[24] It is also worth to emphasize that, as shown above (Figure 3), LA conversion for Ru/TiO₂ catalysts leveled off upon recycling, which might suggest that a semipermeable, equilibrium state is reached for the formed amorphous overcoat. Indeed, the overlayer originating from A-SMSI was thought to be porous enough to allow molecules to interact with the metal surface in the work of Matsubu *et al.*^[24]

While the mechanism of A-SMSI formation is still unclear, several similarities with monocarboxylic acid-induced oxygen vacancy formation on titania can be discerned.^[63,64] For example, formic acid is known to adsorb dissociatively on TiO₂, with dissociated protons combining with nearby bridging oxygens, producing bridging hydroxyl groups, followed by H₂O dissociation and oxygen vacancy formation.^[62,63] This finally results in a HCO_x-covered, disordered and reduced titania surface. Such a disordered surface on TiO₂ (110) was also reported by Henderson with the help of High-Resolution Electron Energy Loss Spectroscopy (HREELS) after formic acid decomposition, as a result of bridging surface hydroxyl group condensation.^[62] White *et al.* further demonstrated that the thermal decomposition of trimethylacetic acid on TiO₂ largely mirrored that of formic acid, also generating oxygen vacancies on the surface of TiO₂ material as revealed by ¹⁸O isotope labelling experiments.^[65] Based on those studies and the experimental results presented above, it is hypothesized that an adsorbate-induced SMSI rather than a direct support reduction resulting from classical H₂ spillover occurred under the mild liquid LA hydrogenation conditions and that the organic acid substrate LA plays a key role in this process.

Long-term Catalyst Stability

As discussed above, the rutile supported catalyst is most stable against deactivation by A-SMSI support reduction when used in a batch reactor in dioxane. To assess longer term stability performance of the Ru/TiO₂ catalysts, the materials were tested in a continuous flow reactor under similar dioxane LA hydrogenation conditions (Figure 4). Similar to the catalytic results obtained for the batch reactions, the initial catalytic activity of the catalysts follows the order: Ru/Anatase > Ru/Rutile > Ru/P25. The LA conversion decreased continuously and significantly for Ru/P25 and Ru/Anatase (Figure 4), in line with the observations made for the recycling tests in batch. Interestingly, Ru/P25 and Ru/Anatase exhibited a similar catalytic activity after 20 h reaction, even though big differences in initial catalytic

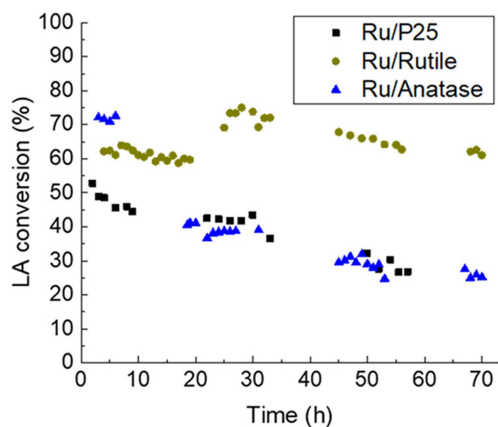


Figure 4. LA conversion as a function of time over Ru/P25, Ru/Rutile and Ru/Anatase. Experimental conditions: $T = 150^{\circ}\text{C}$, $P(\text{H}_2) = 30$ bar and $t = 72$ h, $\text{WHSV} = 1.2 \text{ g}_{\text{LA}} \text{ g}_{\text{catalyst}}^{-1} \text{ h}^{-1}$, upflow configuration.

efficiency were seen. In contrast, a jump in LA conversion was again seen for Ru/Rutile, similar to the increase seen in batch recycling, after which a slow decrease in activity was noted. The origin of this jump is as of yet unclear, but can be speculatively attributed to the microstructural evolution of catalyst^[24] and/or a beneficial effect resulting from a limited SMSI.^[33–36] It also worth to notice that with longer time-on-stream all catalysts exhibited the same slope of deactivation, suggesting that gradual coke buildup causes this gradual deactivation, after an equilibrium in terms of SMSI coverage is reached. Indeed, also after 72 h time-on-stream, no obvious metal sintering was observed for spent Ru/P25 and Ru/Rutile catalysts (Figure S3). Overall, the continuous flow results also show that Ru/Rutile performed better than the (mixed)anatase supported catalyst materials.

Conclusions

The effect of TiO_2 support type on Ru catalyst performance under typical LA hydrogenation reaction conditions was examined, using rutile, anatase and the mixture of these two titania phases, i.e. P25, as support oxides to disperse the Ru nanoparticles. A set of Ru/ TiO_2 catalysts with similar metal loading and Ru particle size was prepared and their stability assessed by multiple recycling under batch reactor conditions in dioxane. Both the benchmark catalyst Ru/P25 as well as Ru/Anatase showed a continuous decrease in GVL yield upon recycling. In contrast, the rutile-supported material performed better under the applied conditions, both in batch as well as in a continuous flow experiment. Characterization by TEM, TGA, FT-IR spectroscopy after CO adsorption demonstrated that the observed deactivation for (mixed) anatase supported catalysts can be attributed to Strong Metal Support Interaction (SMSI) formation rather than coke formation or metal sintering, with the rutile phase proving more resilient against such support reduction. The surprising SMSI effect seen under the applied, relatively mild conditions is shown to require an organic acid,

such as LA and valeric acid, to be present, suggesting that these organic acids play a key role in the eventual support reduction and metal overcoating. These results clearly show that catalyst performance highly depends on the support structure and are useful for the selection of efficient catalysts for catalytic biomass conversion processes. Further systematic studies are now needed of the exact nature of observed A-SMSI formation under these mild, liquid phase hydrogenation conditions.

Experimental Section

Catalyst Synthesis

All chemicals were used as received. For catalyst preparation: ruthenium(III) nitrosyl nitrate ($\text{RuNO}(\text{NO}_3)_3/\text{Ru}$ 31.3%) and $\text{RuCl}_3 \cdot x\text{H}_2\text{O}$ were purchased from Alfa Aesar and Sigma-Aldrich, respectively. The support TiO_2 (P25) was purchased from Degussa, while TiO_2 (rutile, nanopowder, < 100 nm particle size, 99.5% trace metals basis) and TiO_2 (anatase) were obtained from Sigma-Aldrich. For the catalytic tests: levulinic acid (98%), 1,4-dioxane (99+%, containing 0.05% of H_2O) were obtained from Alfa Aesar. Anisole (99%), used as an internal standard, was purchased from Acros Organics. Technical grade acetone ($> 99\%$), used for washing the catalyst, was purchased from Interchemia.

Preparation of 1 wt.% Ru/P25 and Ru/Rutile. The catalysts were prepared via wet impregnation following a previous report.^[24] In short, the supports were first dried at 120°C for 2 h to remove humidity. Subsequently, a slurry of support and demi-water was stirred at room temperature for 30 min, followed by dropwise addition of 10 mL of a Ru precursor ($\text{RuNO}(\text{NO}_3)_3/\text{Ru}$ 31.3%) solution after which the slurry was stirred for 3 h. After evaporation of the water under vacuum at 60°C , the catalyst was dried at 60°C overnight in air, calcined at 500°C for 3.5 h with a heating ramp of $5^{\circ}\text{C}/\text{min}$ under a pure N_2 flow of 100 mL/min, followed by its reduction at 450°C with a ramp rate of $5^{\circ}\text{C}/\text{min}$, for 5 h, under a pure H_2 flow at 80 mL/min.

Preparation of 1 wt.% Ru/Anatase. The catalyst was prepared following the work of Piskun *et al.*^[47] In a typical experiment, 1 g anatase support was first dried at 120°C for 4 h to remove humidity. The metal precursor ($\text{RuCl}_3 \cdot x\text{H}_2\text{O}$) was dissolved in 25 mL water and stirred for 30 min at 30°C , followed by a gradually addition of support to the precursor solution under stirring. Afterwards, the temperature was heated to 85°C and kept at this temperature until all water was evaporated. Subsequently, the catalysts were reduced directly, i.e. without intermediate calcination, at 450°C with a heating ramp of $2^{\circ}\text{C}/\text{min}$ under a 10% H_2/N_2 flow with a total flow of 200 mL/min.

Catalyst Characterization

X-ray powder diffraction (XRD) patterns were measured using a Bruker-AXS D2 Phaser powder X-ray diffractometer using $\text{Co K}_{\alpha 1,2}$ with $\lambda = 1.79026$ Å. Measurements were carried out between 20 – 55° 2θ using a step size of 0.04° and a scan speed of 1 s.

Transmission Electron Microscopy (TEM) analyses were operated with JEOL 100CX microscope at a 100 kV acceleration voltage. The samples were prepared by applying three drops of a catalyst in ethanol slurry on a graphene-coated, 200 mesh copper grid.

N_2 physisorption isotherms were recorded with a Micromeritics Tristar 3000 setup. The samples were outgassed prior to performing

the measurement overnight at 200 °C in a N₂ flow. Surface areas were determined using the Brunauer-Emmett-Teller (BET) theory.

Fourier-transform infrared (FT-IR) spectra in transmission mode were recorded on a Perkin-Elmer 2000 instrument. Samples were pressed under 3.5 tons for 15 s to achieve self-supporting wafers (12–28 mg/13 mm diameter). The wafer was positioned in a well-sealed cell with CaF₂ window and posteriorly activated at 550 °C (5 °C/min) under high vacuum (10^{−6} mbar). Subsequently, the cell was cooled down to −188 °C with liquid nitrogen. Spectra were taken upon CO (10% in He, purity 99.9%) adsorption on the sample, at elevated pressures.

Thermal gravimetric analysis (TGA) was performed with a Perkin-Elmer Pyris 1 apparatus. 15 mg of catalyst was heated with a ramp of 5 °C/min to 150 °C for 1 h in a 20 mL/min Ar flow to eliminate physisorbed water and acetone remaining from the washing step, followed by a ramp of 5 °C/min to 600 °C in a 10 mL/min O₂ flow to burn off deposited organic species.

Catalyst Performance Testing

All batch reactions were run in a 40 mL Parr batch autoclave for 3 h at a stirring speed of 1250 rpm. In a typical reaction, the batch autoclave reactor was loaded with the catalyst (0.19 g), levulinic acid (3 g, 25.8 mmol) and 1,4-dioxane solvent (27 g). Then the autoclave was purged three times with Ar after which the reaction mixture was heated to 150 °C and charged with 30 bar H₂.^[24] This was taken as the starting point of the reaction. During the reaction, samples were collected at different intervals, filtered and internal standard (anisole) was added to the samples. After 3 h of reaction, the autoclave was cooled rapidly to room temperature in an ice bath, after which the remaining H₂ was released. The catalyst was separated by filtration (filters of 0.45 μm), washed with acetone and dried overnight at 60 °C in air. One reference run without the addition of levulinic acid was also operated for 18 h under otherwise identical conditions over Ru/P25. The reaction products were analyzed using a Shimadzu GC-2010A gas chromatograph equipped with a CPWAX 57-CB column (25 m × 0.2 mm × 0.2 μm) and FID detector, using authentic samples for calibration.

Continuous flow reactions were performed under identical reaction conditions with a stainless steel, fixed-bed flow reactor (42.5 cm in length, 0.9 cm in outer diameter and 0.8 cm in inner diameter). 0.5 g (70–150 μm) of catalyst was packed in the center of the reactor tube and plugged with quartz wool. Prior to heating, H₂ pressure was built up slowly by flowing 100 Standard Cubic Centimeter per Minute (sccm) of pure H₂ gas to 30 bar, after which the H₂ flow kept as 10 sccm. Then 10 wt.% LA/dioxane feedstock was introduced into the reactor in an upflow configuration by an HPLC pump with a weight hourly space velocity of 1.2 g_{LA} g_{catalyst}^{−1} h^{−1} and the system was heated to 150 °C with a ramp of 2 °C/min. Once the temperature reached the desired value, this was taken as the starting point of the reaction. Samples of the product solution were taken manually and analyzed offline on a Shimadzu GC-2010A gas chromatograph.

Acknowledgements

The authors gratefully acknowledge the China Scholarship Council (CSC) as well as the Netherlands Center for Multiscale Catalytic Energy Conversion (MCEC), an NWO Gravitation programme funded by the Ministry of Education, Culture and Science of the government of the Netherlands. The authors would also like to

thank Pasi Paalanen, Nazila Masoud, Wouter Lamme and Mark Meijerink (all from Utrecht University) for technical support.

Conflict of Interest

The authors declare no conflict of interest.

Keywords: Biomass · catalyst deactivation · hydrogenation · support reduction · titanates

- [1] W. R. H. Wright, R. Palkovits, *ChemSusChem* **2012**, *5*, 1657–1667.
- [2] S. De, B. Saha, R. Luque, *Bioresour. Technol.* **2015**, *178*, 108–118.
- [3] J. Ftouni, H. C. Genuino, A. Muñoz-Murillo, P. C. A. Bruijninx, B. M. Weckhuysen, *ChemSusChem* **2017**, *10*, 2891–2896.
- [4] J. P. Lange, R. Price, P. M. Ayoub, J. Louis, L. Petrus, L. Clarke, H. Gosselink, *Angew. Chem. Int. Ed.* **2010**, *122*, 4479–4483.
- [5] M. A. Mellmer, C. Sener, J. M. R. Gallo, J. S. Luterbacher, D. M. Alonso, J. A. Dumesic, *Angew. Chem. Int. Ed.* **2014**, *53*, 11872–11875.
- [6] B. L. Oser, S. Carson, M. Oser, *Food Cosmet. Toxicol.* **1965**, *3*, 563–569.
- [7] Z. Zhang, *ChemSusChem* **2016**, *9*, 156–171.
- [8] H. Xiong, S. Lin, J. Goetze, P. Pletcher, H. Guo, L. Kovarik, K. Artyushkova, B. M. Weckhuysen, A. K. Datye, *Angew. Chem. Int. Ed.* **2017**, *56*, 8986–8991.
- [9] F. Liguori, C. Moreno-Marrocan, P. Barbaro, *ACS Catal.* **2015**, *5*, 1882–1894.
- [10] A. M. Ruppert, M. Jędrzejczyk, O. Sneká-Plátek, N. Keller, A. S. Dumon, C. Michel, P. Sautet, J. Grams, *Green Chem.* **2016**, *18*, 2014–2028.
- [11] M. Varkolu, V. Velpula, D. R. Burri, S. R. R. Kamaraju, *New J. Chem.* **2016**, *40*, 3261–3267.
- [12] S. Xu, D. Yu, T. Ye, P. Tian, *RSC Adv.* **2017**, *7*, 1026–1031.
- [13] O. A. Abdelrahman, H. Y. Luo, A. Heyden, Y. Román-Leshkov, J. Q. Bond, *J. Catal.* **2015**, *329*, 10–21.
- [14] A. Piskun, J. Winkelman, Z. Tang, H. Heeres, *Catalysts* **2016**, *6*, 131–151.
- [15] P. P. Upare, J. M. Lee, D. W. Hwang, S. B. Halligudi, Y. K. Hwang, J. S. Chang, *J. Ind. Eng. Chem.* **2011**, *17*, 287–292.
- [16] C. Michel, P. Gallezot, *ACS Catal.* **2015**, *5*, 4130–4132.
- [17] L. E. Manzer, *Appl. Catal. A* **2004**, *272*, 249–256.
- [18] J. Tan, J. Cui, T. Deng, X. Cui, G. Ding, Y. Zhu, Y. Li, *ChemCatChem* **2015**, *7*, 508–512.
- [19] W. Luo, U. Deka, A. M. Beale, E. R. H. van Eck, P. C. A. Bruijninx, B. M. Weckhuysen, *J. Catal.* **2013**, *301*, 175–186.
- [20] J. P. Lange, *Angew. Chem. Int. Ed.* **2015**, *54*, 13186–13197.
- [21] D. Ding, J. Wang, J. Xi, X. Liu, G. Lu, Y. Wang, *Green Chem.* **2014**, *16*, 3846–3853.
- [22] A. M. R. Galletti, C. Antonetti, V. De Luise, M. Martinelli, *Green Chem.* **2012**, *14*, 688–694.
- [23] M. G. Al-Shaal, W. R. H. Wright, R. Palkovits, *Green Chem.* **2012**, *14*, 1260–1263.
- [24] J. Ftouni, A. Muñoz-Murillo, A. Goryachev, J. P. Hofmann, E. J. M. Hensen, L. Lu, C. J. Kiely, P. C. A. Bruijninx, B. M. Weckhuysen, *ACS Catal.* **2016**, *6*, 5462–5472.
- [25] J. Sá, J. Bernardi, J. A. Anderson, *Catal. Lett.* **2007**, *114*, 91–95.
- [26] L. B. Xiong, J. L. Li, B. Yang, Y. Yu, *J. Nanomater.* **2012**, doi: 10.1155/2012/831524.
- [27] Y. Zhu, D. Liu, M. Meng, *Chem. Commun.* **2014**, *50*, 6049–6051.
- [28] S. Tauster, *J. Catal.* **1978**, *55*, 29–35.
- [29] Y. Li, Y. Fan, H. Yang, B. Xu, L. Feng, M. Yang, Y. Chen, *Chem. Phys. Lett.* **2003**, *372*, 160–165.
- [30] Z. Rui, S. Wu, C. Peng, H. Ji, *Chem. Eng. J.* **2014**, *243*, 254–264.
- [31] J. Badyal, *J. Catal.* **1991**, *129*, 486–496.
- [32] M. Sanchez, *J. Catal.* **1987**, *104*, 120–135.
- [33] M. A. Vannice, D. Poondi, *J. Catal.* **1997**, *169*, 166–175.
- [34] D. Poondi, M. A. Vannice, *J. Mol. Catal. A Chem.* **1997**, *124*, 79–89.
- [35] P. Mäki-Arvela, J. Hájek, T. Salmi, D. Y. Murzin, *Appl. Catal. A* **2005**, *292*, 1–49.
- [36] T. Ekou, L. Ekou, A. Vicente, G. Lafaye, S. Pronier, C. Especel, P. Marécot, *J. Mol. Catal. A Chem.* **2011**, *337*, 82–88.
- [37] M. S. Kim, S. H. Chung, C. J. Yoo, M. S. Lee, I. H. Cho, D. W. Lee, K. Y. Lee, *Appl. Catal. B* **2013**, *142–143*, 354–361.

- [38] J. C. Colmenares, A. Magdziarz, M. A. Aramendia, A. Marinas, J. M. Marinas, F. J. Urbano, J. A. Navio, *Catal. Commun.* **2011**, *16*, 1–6.
- [39] O. Dulub, W. Hebenstreit, U. Diebold, *Phys. Rev. Lett.* **2000**, *84*, 3646–3649.
- [40] J. C. Matsubu, S. Zhang, L. DeRita, N. S. Marinkovic, J. G. Chen, G. W. Graham, X. Pan, P. Christopher, *Nat. Chem.* **2016**, *9*, 120–127.
- [41] E. I. Ko, R. L. Garten, *J. Catal.* **1981**, *68*, 233–236.
- [42] M. Bowker, P. Stone, P. Morrall, R. Smith, R. Bennett, N. Perkins, R. Kvon, C. Pang, E. Fourre, M. Hall, *J. Catal.* **2005**, *234*, 172–181.
- [43] M. Bowker, R. Sharpe, *Catal. Struct. React.* **2015**, *1*, 140–145.
- [44] C. Hernandez-Mejia, E. S. Gnanakumar, A. Olivos-Suarez, J. Gascon, H. F. Greer, W. Zhou, G. Rothenberg, N. Raveendran Shiju, *Catal. Sci. Technol.* **2016**, *6*, 577–582.
- [45] J. M. González Carballo, E. Finocchio, S. García, S. Rojas, M. Ojeda, G. Busca, J. L. G. Fierro, *Catal. Sci. Technol.* **2011**, *1*, 1013–1023.
- [46] A. M. Ruppert, J. Grams, M. Jędrzejczyk, J. Matras-Michalska, N. Keller, K. Ostojka, P. Sautet, *ChemSusChem* **2015**, *8*, 1538–1547.
- [47] A. S. Piskun, J. Ftouni, Z. Tang, B. M. Weckhuysen, P. C. A. Bruijninx, H. J. Heeres, *Appl. Catal. A* **2018**, *549*, 197–206.
- [48] T. Ohno, K. Sarukawa, K. Tokieda, M. Matsumura, *J. Catal.* **2001**, *203*, 82–86.
- [49] K. Hadjiivanov, J. C. Lavalley, J. Lamotte, F. Maugé, J. Saint-Just, M. Che, *J. Catal.* **1998**, *176*, 415–425.
- [50] K. Hadjiivanov, J. Lamotte, J. C. Lavalley, *Langmuir* **1997**, *13*, 3374–3381.
- [51] K. Hadjiivanov, *Appl. Surf. Sci.* **1998**, *135*, 331–338.
- [52] L. Mino, G. Spoto, S. Bordiga, A. Zecchina, *J. Phys. Chem. C* **2012**, *116*, 17008–17018.
- [53] D. Liuzzi, F. J. Pérez-Alonso, F. J. García-García, F. Calle-Vallejo, J. L. G. Fierro, S. Rojas, *Catal. Sci. Technol.* **2016**, *6*, 6495–6503.
- [54] T. Xia, C. Zhang, N. A. Oyler, X. Chen, *Adv. Mater.* **2013**, *25*, 6905–6910.
- [55] X. Chen, L. Liu, Z. Liu, M. A. Marcus, W.-C. Wang, N. A. Oyler, M. E. Grass, B. Mao, P.-A. Glans, P. Y. Yu, J. Guo, S. S. Mao, *Sci. Rep.* **2013**, *3*, 1510–1517.
- [56] X. Chen, L. Liu, F. Huang, *Chem. Soc. Rev.* **2015**, *44*, 1861–1885.
- [57] M. Sankar, Q. He, S. Dawson, E. Nowicka, L. Lu, P. C. A. Bruijninx, A. M. Beale, C. J. Kiely, B. M. Weckhuysen, *Catal. Sci. Technol.* **2016**, *6*, 5473–5482.
- [58] J. Robbins, *J. Catal.* **1989**, *115*, 120–131.
- [59] V. A. de la Peña O'Shea, M. Consuelo Álvarez Galván, A. E. Platero Prats, J. M. Campos-Martin, J. L. G. Fierro, *Chem. Commun.* **2011**, *47*, 7131–7133.
- [60] Y. Zhu, D. Liu, M. Meng, *Chem. Commun.* **2014**, *50*, 6049–6051.
- [61] Z. Rui, L. Chen, H. Chen, H. Ji, *Ind. Eng. Chem. Res.* **2014**, *53*, 15879–15888.
- [62] M. A. Henderson, *J. Phys. Chem. B* **1997**, *101*, 221–229.
- [63] C. Lun Pang, R. Lindsay, G. Thornton, *Chem. Soc. Rev.* **2008**, *37*, 2328–2353.
- [64] B. D. Chandler, *Nat. Chem.* **2017**, *9*, 108–109.
- [65] J. M. White, J. Szanyi, M. A. Henderson, *J. Phys. Chem. B* **2004**, *108*, 3592–3602.

Manuscript received: March 12, 2019
 Revised manuscript received: March 5, 2019
 Version of record online: April 2, 2019